Original Article
Optical imaging with a novel cathepsin-activatable probe for enhanced detection of colorectal cancer

Shadi A Esfahani[1], Pedram Heidari[1], Melanie H Kucherlapati[2,3], Jorge M Ferrer[4], Raju S Kucherlapati[2,3], Umar Mahmood[1]

[1]Athinoula A Martinos Center for Biomedical Imaging, Department of Radiology, Massachusetts General Hospital, Charlestown, MA, USA; [2]Department of Genetics, Harvard Medical School, Boston, MA, USA; [3]Department of Medicine, Division of Genetics, Brigham and Women's Hospital Boston, MA, USA; [4]Lumicell, Inc, 275 Washington Street, Newton, MA, USA

Abstract: We evaluated a cysteine cathepsin-activatable optical imaging probe (LUM015) with improved kinetics relative to larger macromolecules for detection and characterization of colorectal cancer (CRC), and thereby assessed its potential use in fluorescence-guided colonoscopy. We showed that LUM015 is stable in plasma. In-vitro studies demonstrated selectivity of LUM015 for targeting cathepsins; there was robust increase in emitted fluorescence signal from the cathepsin overexpressing HT-29 CRC cells within 1-5 minutes after incubation with LUM015 compared to the cells incubated with combination of LUM015 and a pan-protease inhibitor (as negative control). Biodistribution, differential accumulation of the probe in the tumor and tumor-to-background fluorescence signal ratio of LUM015 were compared to ProSense680, a commercially available protease-activatable optical imaging probe, over 24 hours after intravenous injection of the probes in nude mice with subcutaneously implanted HT-29 tumors. LUM015 showed distinct kinetics compared to ProSense680 with time to peak signal for subcutaneous tumor-to-colon ratio of 3.3±0.3 (mean ± SD) at 4-8 hours compared to 2.9±0.2 at 24 hours, respectively (n=8 for each group). Near-infrared fluorescence imaging and dual channel colonoscopy of the mice with orthotopic colon tumors showed tumor-to-colon ratio of 3.7±0.2 in HT-29 tumors (n=4), 2.8±0.1 in genetically engineered mice with APC^{KO}Kras$^{LSL-G12D}$p53$^{flox/flox}$ mutation (n=4), and 4.1±0.1 in mice with APC$^{LoxP/LoxP}$Msh2$^{LoxP/LoxP}$ mutation (n=4) at 6 hours after LUM015 administration. Immunohistochemistry and laser confocal microscopy of the extracted tumors confirmed high expression of cysteine cathepsins in all colon tumor types tested. Optical imaging with cathepsin-activatable LUM015 in multiple models of CRC highlights its potential for increasing the efficacy of CRC screening and therapeutic procedures.

Keywords: Cathepsin, activatable probe, colorectal cancer, optical imaging, tumor detection

Introduction

Colorectal cancer (CRC) is the third most common cancer worldwide and despite marked advances in diagnosis and management, it is the fourth most common cause of cancer-related mortality with global incidence rate of 1.65 million new cases and 835,000 deaths per year [1]. Colonoscopy is the routine method of CRC screening with overall excellent diagnostic performance and has been shown to reduce CRC mortality [2]. However, it has lower sensitivity for detection of small polyps at early stages with reported approximately up to 20% miss rate for colonic polyps [3]. Therefore, there is

an unmet clinical need for development of novel imaging techniques for improved detection and real-time evaluation of the neoplastic processes in the colon and ultimately increasing the efficiency of endoscopic screening procedures.

Optical molecular imaging is a technology that enables early detection and characterization of CRC, and assessment of the response to therapeutic interventions [4, 5]. Previous studies have shown that optical imaging using non-specific organic fluorophores such as methylene blue and indocyanine green can be used for localization of detection of primary and metastatic CRC with high sensitivity and tumor-to-
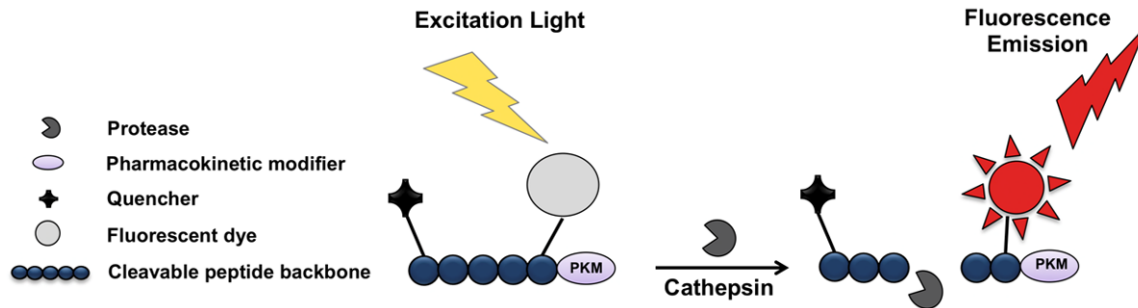
Figure 1. Schematic structure of LUM015. The probe consists of a fluorescence quencher molecule (QSY21) attached to a 20-kD polyethylene glycol (PEG) as a pharmacokinetic modifier, and a Cy5 fluorophore through a GGRK peptide. Once the proteolytic enzyme cleaves the quencher, the optically active fragment is released.

background ratio (TBR) [6, 7]. However, these probes are non-specific for neoplastic lesions and the increase in local fluorescence signal is mainly driven by increase in blood flow and leakiness of the tumor vessels; therefore, these probes do not provide specific information for in-situ characterization of the tumors. Multiple molecularly targeted optical imaging agents have been developed which target enzymes such as proteases [5, 8], reporters of apoptosis [9], or angiogenesis processes [10] among others. Cysteine cathepsins are a group of lysosomal proteases, which have received much attention as molecular targets for detection of various types of tumors including CRC. Overexpression of multiple cysteine cathepsins including K, L, S and B has been shown to be associated with CRC tumor progression, metastasis and shortening of patients' survival by facilitating the invasion of cancer cells, endothelial and inflammatory cells, and progression of necrotic and apoptotic cell death [11-14]. Studies have reported that highly selective inhibitors of cathepsins result in suppression of CRC invasion and metastasis [15, 16]. Thus, a cathepsin-targeting probe could provide a minimally invasive strategy for improved diagnosis of CRC.

LUM015 (Lumicell, Newton, MA) is an optical molecular imaging probe highly selective for cysteine cathepsins with improved kinetics compared to larger macromolecular agents, which has undergone phase 1 human safety testing and has demonstrated the potential for translation in a variety of applications [17, 18]. In this study, we assessed the LUM015 probe for early detection and precise characterization of the tumors in multiple mouse models of CRC. In addition, biodistribution and specificity of the LUM015 probe for detection of CRC

was compared to Prosense680, a commercially available protease-activatable probe.

Materials and methods

Optical imaging probe (LUM015)

LUM015 is a novel protease-activatable optical imaging probe, which consists of a fluorescence quencher molecule (QSY21) attached to a 20-kD polyethylene glycol (PEG) and a Cy5 fluorophore through a GGRK peptide [17]. Once the proteolytic enzyme cleaves the peptide backbone and removes the quencher, the optically active fragment is released (**Figure 1**). In-vitro studies have shown that this peptide is activated by different types of cysteine cathepsins including cathepsin K, L, S, and B [17]. Preclinical toxicity studies of LUM015 performed in rats and dogs indicated a wide margin of safety. This probe has undergone phase 1 human safety testing in a pilot study on patients with breast cancer or soft tissue sarcoma. LUM015 biodistribution, pharmacokinetic profiles, and metabolism have been comparable in mice and human subjects [17, 19].

Assessment of the stability of LUM015 probe in plasma

To assess the stability of LUM015 probe in the murine plasma, the probe (4 nmol/150 μl, 27 μM) was mixed with 150 ml of either Dulbecco's Phosphate Buffered Saline (D-PBS, ATCC) as negative control, Trypsin (ATCC) as positive control, or murine plasma. The mixtures were incubated in 37°C for 6 hours. The mean fluorescence intensity (MFI) of each sample was measured over time using the Carestream In-Vivo Multispectral FX imaging system (NYC, USA)

with excitation filter of 650 nm and emission filter of 700 nm.

Cell culture and western blotting

Human colon cancer cells, HT-29 (ATCC) were cultured in McCoy's 5a medium containing 10% fetal bovine serum, and 1% Penicillin-Streptomycin (ATCC) at 37°C in a humid atmosphere containing 5% CO_2 and 95% air. Western blotting was performed to measure the expression level of multiple cathepsins including cathepsin B, S, L and K in HT-29 cells, using methods previously described [20]. Briefly, after electrophoresis using polyacrylamide gels (Bio-Rad Hercules, USA), proteins were transferred to a polyvinylidene difluoride (PVDF) membrane (Roche, Germany). The membrane was blocked with Tris-buffered saline (10 mM Tris-HCl, pH 8.0, 150 mM NaCl), 0.05% Tween-20 and 5% non-fat dry milk (Bio-Rad). The blot was incubated overnight at 4°C with mouse anti-cathepsin antibodies (Abcam, USA) at 1:1000 dilution, and rabbit beta-actin monoclonal antibody (Santa Cruz, USA) with 1:1000 dilution as an internal control. The membrane was incubated with secondary antibodies of goat anti-mouse IgG-HRP (Santa Cruz) with 1:500 dilution for cathepsin and goat anti-rabbit IgG-HRP antibody (Santa Cruz) with 1:1000 dilution for beta-actin. The bands were detected using enhanced BM Chemiluminescence (Mouse/Rabbit) Western Blotting Kit (Roche). Quantitation of cathepsin and beta-actin expression was performed by drawing a region of interest over the protein bands on the images using the Carestream analysis software. The measured level of cathepsin expression was normalized to the beta-actin level.

In vitro assessment of LUM015 probe for targeting cathepsins

For *in vitro* assessment of the cellular fluorescence in the presence of LUM015, HT-29 cells were cultured on sterile coverslips in 6-well plates. After two days, media was removed from the wells. The cells were incubated with LUM015 probe (27 µM) or a mixture of the probe and a pan-protease inhibitor (Sigma-Aldrich, USA) at 37°C for 5 minutes. The fluorescent signal emitted from the cancer cells and extracellular space was qualitatively assessed under a laser scanning confocal micro-scope (LSM-5 PASCAL, Zeiss, Germany) with emission wavelength of 633 nm.

Mouse models of colorectal caner

All animal experiments were approved by our Institutional Animal Care and Use Committee. The subcutaneous tumor-bearing mouse model of CRC was generated by injection of a mixture of $1×10^6$ HT-29 cells with 10% Matrigel (Becton-Dickinson, USA) into the subcutaneous space of the nu/nu mice (Taconic, Germantown, NY; n=16) using a 25-gauge needle. Observation of a bulge under the skin was a sign of successful injection. Tumor growth was monitored weekly and imaging was performed when the tumors reached 7-10 mm in size in approximately 3 weeks.

Additionally, 3 orthotopic mouse models of colon cancer were generated: 1) HT-29 cells were injected into descending colon wall of nude mice (n=4). For this purpose, 250,000-300,000 cells (20-30 µl) were washed with sterile PBS and injected into the wall of the descending colon using a 32-gauge needle. Observation of a small bulge at the site of injection was considered as the sign of successful implantation. 2) A genetically engineered mouse model (GEMM) of orthotopic CRC with common mutations was developed with crossing APC[KO], Kras[LSL-G12D] and p53[flox/flox] mice to generate APC[KO]Kras[LSL-G12D]p53[flox/flox] (AKP) model (n=4). Colonic tumors were induced through focal administration of adenovirus expressing cre recombinase (AdCre) in the descending colon to cause the recombination based on the previously described method [21]. 3) Another GEMM of orthotopic CRC was developed by focal injection of AdCre in the distal colon wall of APC[LoxP/LoxP]Msh2[LoxP/LoxP] mice (3 mice with 4 developed tumors) using previously described method [22].

Development and growth of the orthotopically implanted colon tumors were monitored for 6-8 weeks by weekly colonoscopy until the tumors reached 3-7 mm in largest diameter.

In vivo targeting of cathepsins

In vivo assessment of LUM015 probe was performed in colorectal tumor bearing mice when the tumors reached the appropriate size (7-10 mm for subcutaneous tumors and 3-7 mm for

orthotopic tumors). Mice were anesthetized by inhalation of 100% oxygen and isoflurane (5% for induction and 1.5% for maintenance) via facial mask. The LUM015 probe was prepared with concentration of 3.5 mg/kg based on previous preclinical studies [17], and was injected into the lateral tail vein of the mice (<0.2 ml volume).

Pharmacokinetics of LUM015 in comparison to ProSense680

Mice with subcutaneous HT-29 tumors were imaged using Carestream Multispectral imaging system (Excitation: 570-650 nm, emission: 700 nm) at multiple time points between 5 minutes to 24 hours after injection of LUM015 (n=8). The mean fluorescence signal intensity of the tumors was assessed over the skin and tumor-to-skin (as background) ratio was calculated. These results were compared to a second group of mice with subcutaneous HT-29 tumors (n=8), which were imaged with ProSense680 (Perkin Elmer, USA), a commercially available protease-activatable probe, with concentration of 2 nmol/mouse [23].

Mice from both LUM015 and Prosense680 groups were then euthanized at 6 hours and 24 hours post-injection (n=4 for each group and each time point) and biodistribution of the probes was assessed by comparison of MFI of the tumors and multiple extracted tissues.

Dual channel colonoscopy

Based on the results of LUM015 probe kinetics experiments, *in vivo* optical colonoscopy of the mice with orthotopic CRC was performed at the time point with maximum TBR. The optical endoscopy system was constructed in a manner analogous to the previously designed devices by our group, to incorporate quantitative real-time fluorescence imaging [24, 25]. This custom-designed dual channel apparatus allows simultaneous white light and near-infrared fluorescence (NIRF) imaging. White light was filtered by a dichroic mirror and short-pass filter for wavelengths above 650 nm. For NIRF imaging, we used a fiber coupled 650 nm class IIIb laser (B&W TEK) for excitation and a long-pass emission filter of 700 nm. Mice were given a chlorophyll-free diet for at least one week prior to colonoscopy to minimize the autofluorescence related to ingested material in the

gastrointestinal tract. Under inhalation anesthesia (1.5% vaporized isoflurane in 100% O_2), the endoscope was inserted rectally, air was insufflated through the working channel, and the number and signal of the tumors were assessed. Using the 8-bit white light and NIRF images in ImageJ, a straight line was placed over the regions of interest and the plot profile of the arbitrary signal intensity values was generated. The tumor and adjacent normal colon signals were measured and compared between the images of white light (as conventional method of colonoscopy) and NIRF colonoscopy.

Ex vivo near-infrared fluorescence imaging of colorectal cancer

Mice with orthotopic HT-29 tumors, AKP mutant and $APC^{-/-}Msh^{-/-}$ tumors were euthanized at 6 hours after intravenous injection of LUM015 and the tumor and colon tissues were imaged using the Carestream surface reflectance fluorescence imaging system. The MFI was measured by drawing a 3 mm circular region of interest (ROI) over the respective brightest fluorescence area in the tumors (n=4 for each group) to calculate the mean pixel intensity using standard Carestream image analysis software. Tumor-to-colon ratio was then computed by dividing the MFI of tumor by MFI of adjacent normal colon tissue.

Confocal microscopy and histopathological analysis

The excised tumor tissues were frozen with liquid nitrogen and stored at -80°C. Serial cryostat sections with 5 μm thickness were prepared for H&E & IHC staining, and for qualitative assessment of the tumor fluorescence signal under laser confocal microscopy (LSM-5 PASCAL, Zeiss, Germany, emission wavelength: 633 nm). IHC staining was performed for assessment of cathepsin expression in colon tumor tissues, using the previously described method [20, 26]. In brief, tissue slides were fixed in 100% acetone in -20°C for 10 minutes and left at room temperature for complete evaporation of acetone. The specimens were then incubated with primary anti-cathepsin antibodies specific for cathepsin B, L, S or K (abcam) at 4°C overnight. After incubation with Envision + System-HRP Labeled Polymer anti-rabbit/antmouse (Dako) for 1 hour at room temperature, slides were treated with liquid DAB plus sub-
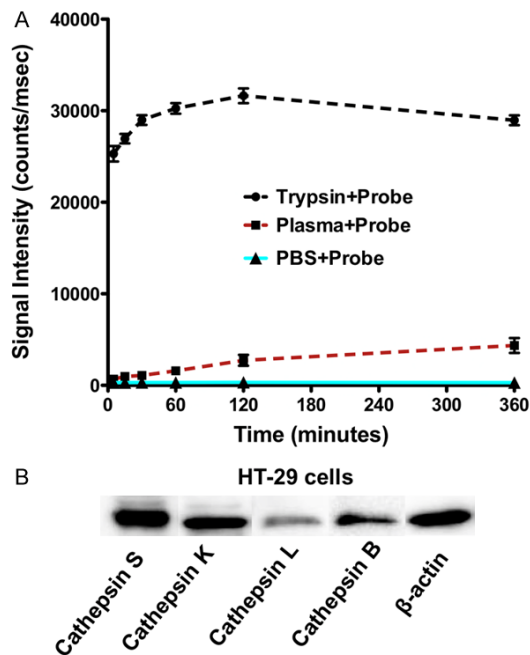
Figure 2. Stability of cathepsin-activatable LUM015 probe in plasma and western blot analysis of cathepsin expression in colorectal cancer cells. A. Incubation of LUM015 probe with trypsin resulted in rapid activation of the probe and robust increase in fluorescence signal intensity. The signal intensity of the probe mixed with murine plasma did not significantly increase over 6 hours compare to the mixture of probe with PBS as negative control. B. Western blot analysis of the HT29 cells showed high expression of cathepsin S, B, K and to lesser degree cathepsin L.

strate chromogen (Dako) and then counterstained with hematoxylin.

Statistical analysis

Statistical analysis was performed using GraphPad Software (version 6, CA, USA). The continuous variables are presented as mean ± standard deviation (SD). Two-tailed Student's *t* test was performed to compare the means of two groups. *P-value* of less than 0.05 was considered as statistically significant.

Results

Stability of cathepsin-activatable probe in murine plasma

We tested the stability of LUM015 probe in plasma to ensure that there is no non-specific activation of the probe by the plasma. While incubation of LUM015 with trypsin showed

rapid activation of the probe and robust increase in the signal intensity of the sample, the fluorescence signal intensity in the mixture of probe with murine plasma remained low with no significant increase over time compared to the mixture of probe and PBS as negative control (**Figure 2A**).

Cathepsin expression level and in vitro assessment of LUM015 fluorescence signal

Western blot analysis demonstrated high expression of cathepsin S, K, B and to lesser extent cathepsin L in HT29 CRC cells (**Figure 2B**). Incubation of the cells with LUM015 showed rapid activation of the probe and increase in fluoresce signal intensity in the cells and extracellular space within 1-5 minutes. However, in the presence of a pan-protease inhibitor cocktail there is no detectable fluorescence signal above the background level with LUM015 (**Figure 3**).

Optimizing the timing for in vivo imaging of LUM015 and comparison of the kinetics of LUM015 and Prosense680

Multispectral deconvolution fluorescence imaging of the mice with subcutaneous HT-29 tumors showed a gradual increase in MFI of the tumors with the maximal tumor-to-skin ratio of 1.8±0.2 at 4-8 hours after intravenous injection of the probe and a slow decline in tumor-to-skin ratio to 1.5±0.1 at 24 hours post injection (**Figure 4A**, **4B**). In comparison to Prosense680, the MFI and tumor-to-skin ratio were higher with LUM015 over 24 hours post-injection (*P*<0.05 from 1-24 hours). The overall kinetics of Prosense680 was much slower in the subcutaneous xenografts and tumor-to-skin ratio reached the peak (1.3±0.1) at 24 hours post injection (**Figure 4B**).

Comparison of biodistribution of LUM015 and ProSense680 in colorectal tumor-bearing mice

Biodistribution of the optical imaging probes at 6 and 24 hours post injection demonstrated more rapid kinetics of LUM015 compared to ProSense680 with faster clearance of LUM015 from background tissues (**Figure 4C**, **4D**) and higher net fluorescence signal intensity in the HT-29 tumors at both time points. In the ProSense680 group, there was higher MFI in multiple excised non-target organs such as liver
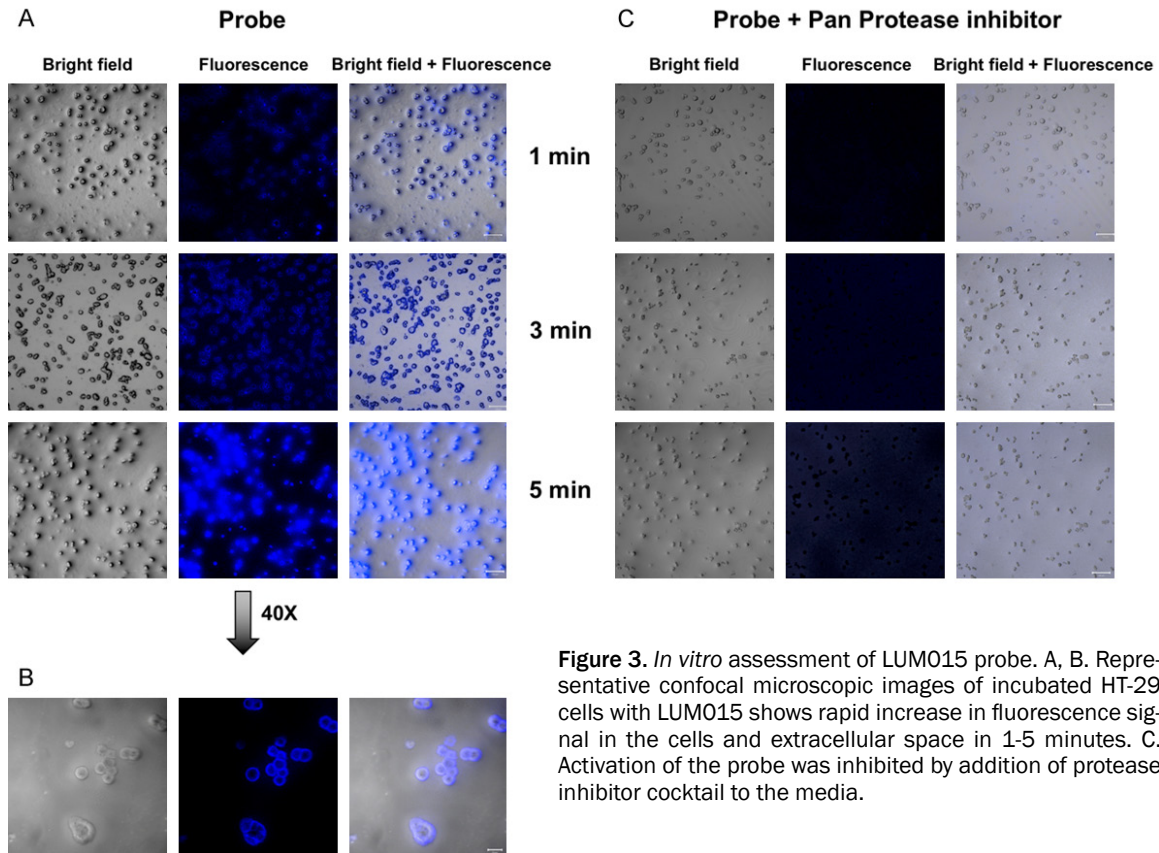
A **Probe**

Bright field | Fluorescence | Bright field + Fluorescence

1 min

3 min

5 min

40X

B

C **Probe + Pan Protease inhibitor**

Bright field | Fluorescence | Bright field + Fluorescence

Figure 3. *In vitro* assessment of LUM015 probe. A, B. Representative confocal microscopic images of incubated HT-29 cells with LUM015 shows rapid increase in fluorescence signal in the cells and extracellular space in 1-5 minutes. C. Activation of the probe was inhibited by addition of protease inhibitor cocktail to the media.

and spleen. Both protease-activatable probes were mainly excreted through the renal system. **Figure 4D** shows representative images of LUM015 and ProSense680 biodistribution at 6 hours post injection.

Comparison of the tumor-to-colon ratio showed higher TBR in LUM015 group compared to Prosense680 (3.3±0.3 vs. 2.1±0.1, respectively, *P*<0.05) at 6 hours post injection. The tumor-to-colon ratio overall decreased in both groups at 24 hours with higher TBR in Prosense680 group compared to LUM015 (2.2±0.1 vs. 2.9± 0.2, respectively, *P*<0.05) (**Figure 4C**).

Fluorescence imaging in orthotopic murine models of colorectal cancer

Based on the probe kinetics simultaneous, white-light and NIRF colonoscopy of the mice with orthotopic colon tumors were performed at 6 hours post-injection. In both orthotopically implanted and genetically engineered mouse models of CRC, tumors were detected with sharp margins and significantly higher tumor-to-colon signal ratio in optical colonoscopy images compared to the conventional white light colonoscopy images (**Figure 5**). Representative analysis of the arbitrary signal of HT-29 tumor and normal adjacent colon tissue is demonstrated on **Figure 5B** and **5C**. Surface reflectance epifluorescence imaging of the extracted colon tumors confirmed our colonoscopy results; high signal intensity was detected in the tumors with tumor-to-colon ratio of 3.7±0.2 (mean ± SD) in mice with orthotopic HT29 tumors, TBR of 2.8±0.1 in AKP mice, and 4.1±0.1 in APC$^{LoxP/LoxP}$Msh2$^{LoxP/LoxP}$ mice at 6 hours post-injection (**Figures 5**, **6**).

Confocal microscopy and histopathological analysis of colorectal tumors

H&E staining of all tumor tissue sections showed well-developed tumors in the subcutaneous space or within the colon wall. Confocal microscopy of the frozen subcutaneous and orthotopic tumor tissues showed high concordance between the areas of increased cysteine cathepsin expression and enhanced fluorescence signal in the tumors while normal adjacent colon tissues showed minimal cathepsin
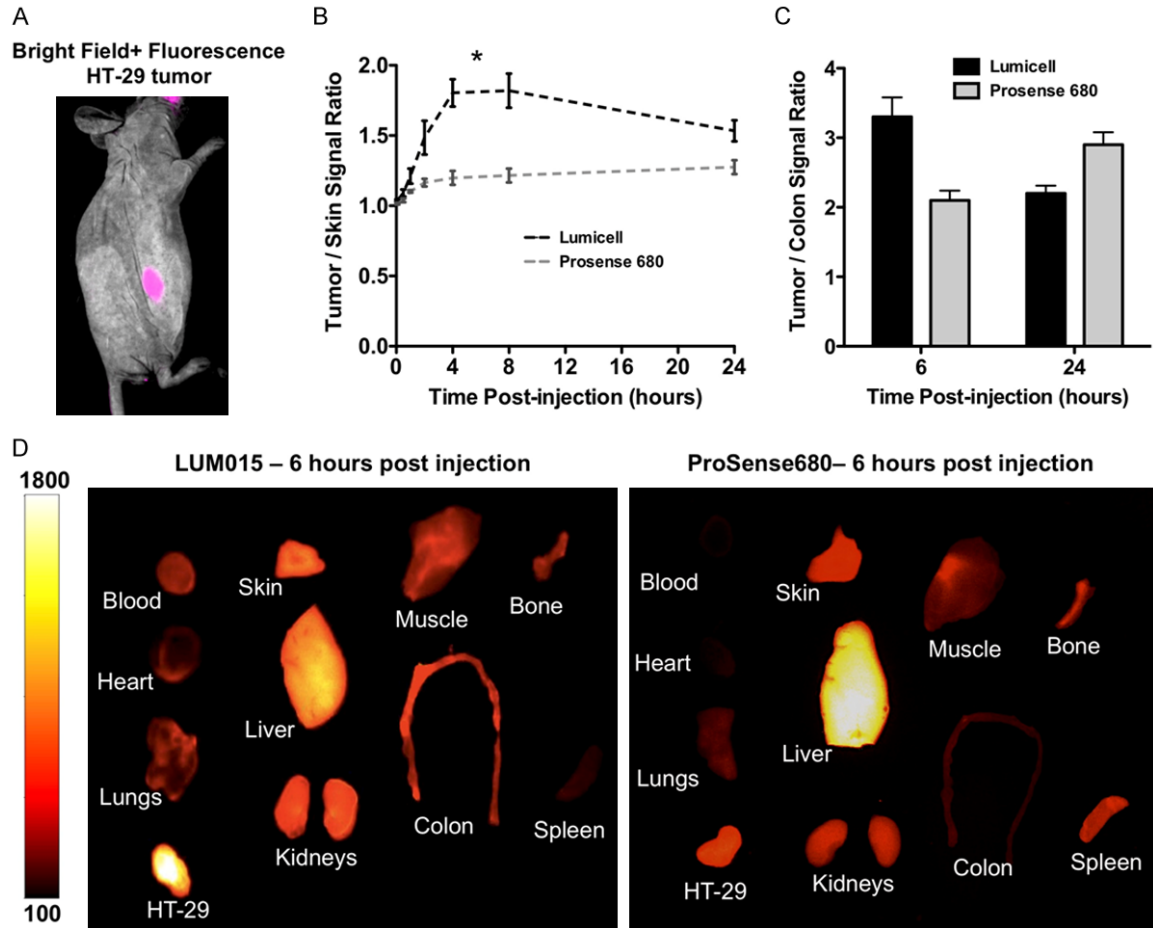
Figure 4. Optimizing the timing for *in vivo* imaging of LUM015 and comparison of the biodistribution of LUM015 and Prosense680. A. Representative multispectral deconvolution fluorescence imaging of the subcutaneously implanted HT29 tumor overlaid with white light at 6 hours post LUM015 injection showed localization of the tumor with sharp margins. B. LUM015 showed overall more rapid kinetics compared to Prosense680 over 24 hours post injection with maximum tumor-to-skin ratio of 1.8±0.2 (mean ± SD) at 4-8 hours (*), and slowly decreased ratio to 1.5±0.1 at 24 hours. C. LUM015 results in maximum tumor-to-colon ratio of 3.3±0.3 at 6 hours, compared to Prosense680, which results in maximum ratio of 2.9±0.2 at 24 hours. D. Representative comparison of LUM015 and ProSense680 biodistribution at 6 hours shows more rapid clearance of LUM015 from non-targeted background tissues such as liver and spleen and higher probe accumulation in the colon tumor compared to Prosense680.

expression and very weak fluorescence signal (**Figure 7**).

Discussion

We demonstrated the use of a cathepsin-activated optical probe for improved detection of small colonic lesions and in-situ characterization of the neoplastic tissues in real-time with high tumor to normal adjacent colon ratio. Upregulation of cysteine cathepsins has been reported in colorectal tumors with common genetic mutations such as APC and Kras genes and microsatellite instability among others [10, 27-29]. Our histopathological analysis con-

firmed overexpression of cysteine cathepsins in multiple mouse models of CRC with either xenografts or spontaneously developed tumors in genetically engineered mouse models. *In vivo* optical imaging of CRC using LUM015 showed selective targeting and accumulation of the probe in the neoplastic tissues resulting in sharp demarcation of the tumor margins. Dual channel colonoscopy system with combination of a NIRF for detection of the molecularly targeted optical probe and conventional colonoscopy is a powerful tool for improved detection of the colonic lesions specifically the small, flat or depressed lesions with malignant potential that can be missed by conventional white light
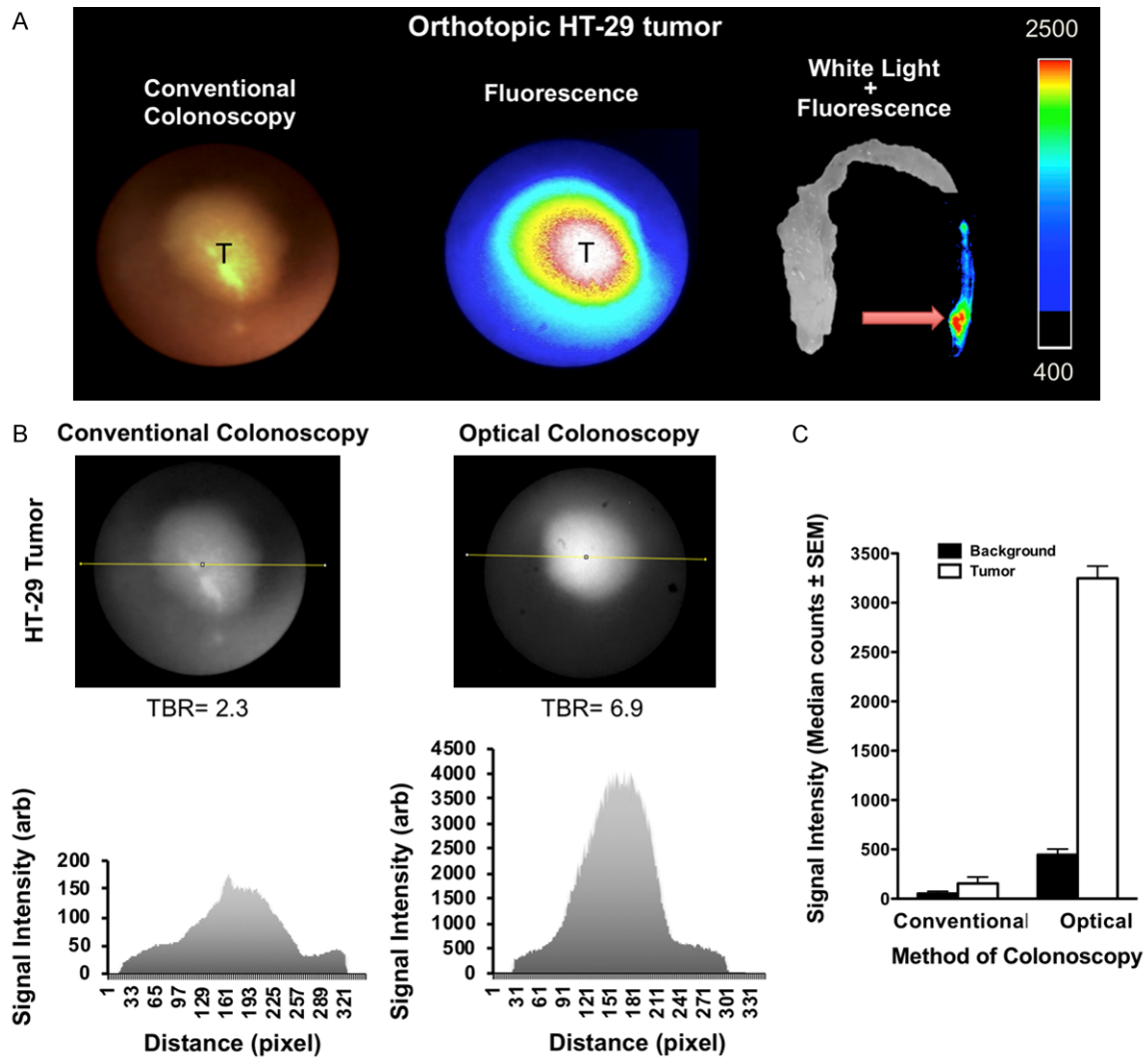
Figure 5. Near-infrared fluorescence imaging and dual channel colonoscopy in orthotopic HT-29 tumors using LUM015. A. Custom-made dual channel colonoscopy using the standard white light and near infrared fluorescence channel detects the implanted HT-29 tumor in distal part of the colon. Surface reflectance epifluorescence imaging of the extracted colon tissue confirms the colonoscopy results with tumor-to-colon ratio of 3.7±0.2 (mean ± SD) at 6 hours post injection. B, C. Representative analysis of the arbitrary signal of the HT-29 tumor and normal adjacent colon tissue demonstrates significantly higher tumor-to-colon ratio in optical image compared to conventional white light (median ± SEM: 7.3±0.2 vs. 2.9±0.3 respectively, $P<0.05$). C: normal adjacent colon background, T: tumor.

colonoscopy [30]. In addition, the standard of care colon lesion biopsy and resection is imprecise in distinguishing neoplastic tissue from surrounding normal colon parenchyma at the tumor margins [4]. Optical imaging with cathepsin-activated targeting probes could provide a real-time method for sensitive detection of the microscopic residual cancer at the tumor margins at the time of surgery, which could reduce the need for re-resection, lower the rates of local recurrence, and personalize adjuvant therapy [19].

Several protease-activated fluorescent imaging probes with different functional characteristics have been developed over the past decade [4, 30]. For instance, MMPSense680, a non-specific near-infrared probe that gets activated by a broad array of matrix metalloprotease (MMP) enzymes [31], and multiple small targeted peptides have been introduced for detection of colonic adenomas and dysplastic lesions [32, 33]. However, these probes require long time to achieve the optimal TBR. ProSense680 is one of the first activatable fluorescence probes that
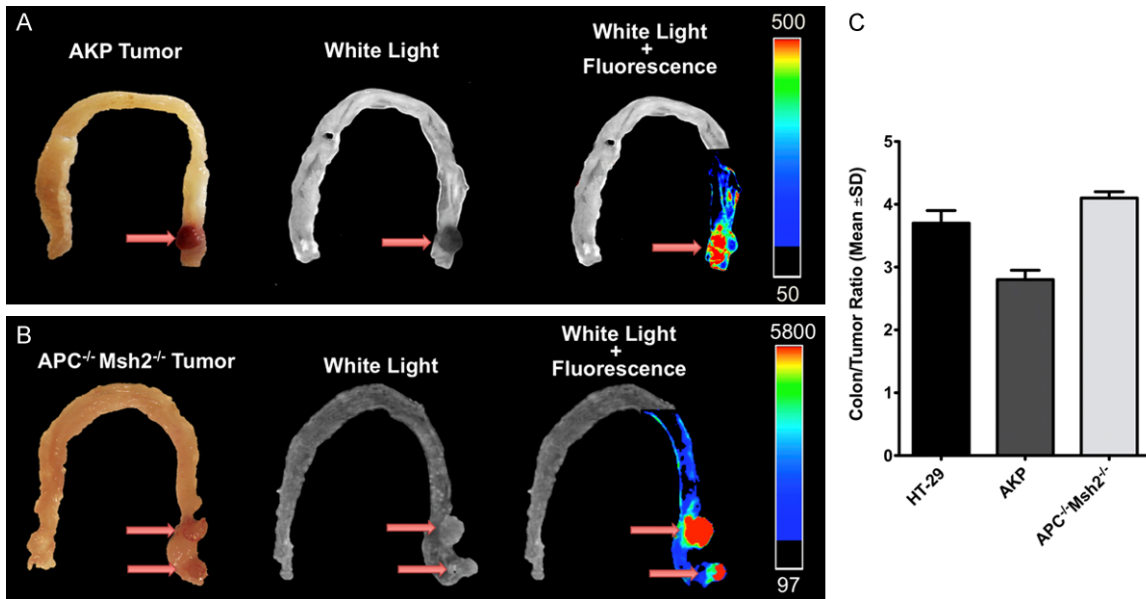
237

Figure 6. Optical imaging of colorectal tumors in genetically engineered mouse models of colorectal cancer. (A) Representative optical imaging of orthotopic colon tumors in 6 hours post probe injection shows significantly increased signal intensity in the tumor relative to the normal adjacent colon tissue with tumor-to-background ratio of 2.8±0.1 in APC^{KO}Kras$^{LSL-G12D}$p53$^{flox/flox}$ (AKP) tumors (A), 4.1±0.1 in APC$^{LoxP/LoxP}$Msh2$^{LoxP/LoxP}$ tumors (B), and 3.7±0.2 in orthotopic HT-29 tumors (C).
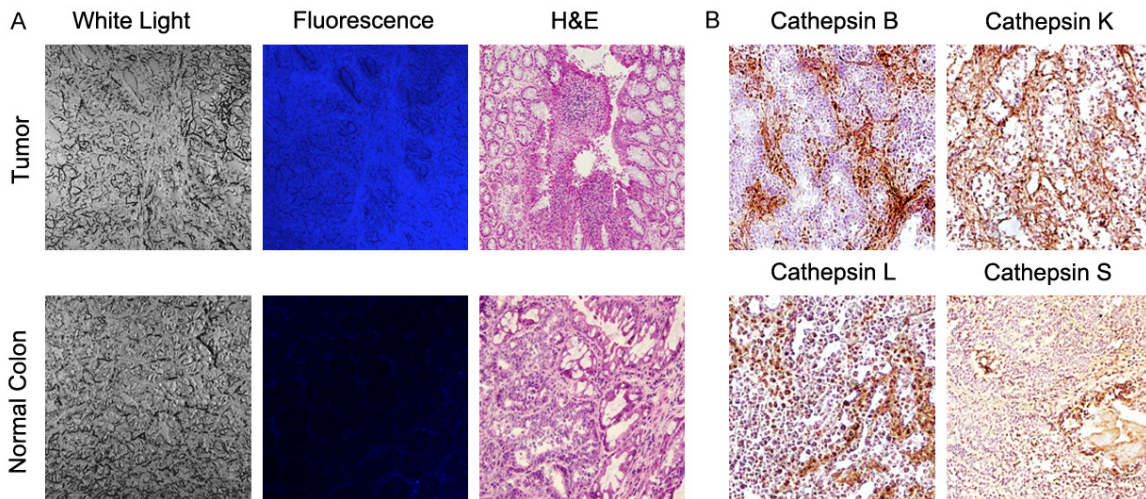

Figure 7. Histopathologic and laser confocal microscopic evaluation of cysteine cathepsins in colorectal cancer. Representative histology and fluorescence confocal microscopy of the tumors in APC$^{LoxP/LoxP}$Msh2$^{LoxP/LoxP}$ mice confirms the results of *in vivo* optical imaging with demonstration of neoplastic cells within different layers of the colon wall with significantly higher fluorescence signal compared to the normal adjacent colon tissue (A), and high expression of cysteine cathepsins S, K, L and B compared to the adjacent normal colon tissue (B).

was introduced for targeting cysteine cathepsins [34] and has shown high signal intensity in different types of cancers including CRC. Our biodistribution studies and comparison of LUM015 with prosense680 demonstrated favorable pharmacokinetics of LUM015 as a low-molecular weight probe with minimal uptake by majority of the relevant background tissues, rapid clearance from normal background colon wall, and rapid accumulation in the tumor. Therefore, LUM015 resulted in higher absolute fluorescence signal intensity in the colon tumors and much shorter time of optimal tumor-to-colon ratio (4-6 hours with LUM015 vs.

24 hours with prosense680). The favorable characteristics of LUM015 potentially facilitates its clinical translation with providing shorter time of dual channel colonoscopy in patients and enabling same day optical-guided procedures such as colonoscopy, biopsy or surgical margin resection. In addition, relatively slow washout of LUM015 from the tumor provides a wide time window for any type of NIRF-guided procedure with single systematic injection of the probe. A recent study by Segal et al, introduced a Cy5-labeled protease activity based probe for detection of colon polyps in APC[min/+] mice [30], which confirms the potential of the activity based probes as promising tools for improving the detection of colorectal lesions using colonoscopy.

To our knowledge, LUM015 is the first protease-activatable probe that has been translated for use in human subjects; a phase-1 clinical safety study on LUM015 (NCT01626066) reported that systemic administration of LUM-015 at 0.5-1.5 mg/kg doses was safe and well-tolerated by patients (n=15) with no adverse reaction or complication [17, 18]. LUM015 is currently under evaluation in feasibility clinical trials for assessment of breast cancer, brain cancer, prostate cancer, peritoneal surface malignancies and gastrointestinal tumors such as colon, esophageal and pancreatic cancers (NCT02438358, NCT03686215, NCT037171-42, NCT03441464, NCT03834272 and NCT-02584244) [35]. A previous study by Lazarides et al, demonstrated that using LUM015 fluorescence-guided laser ablation in mouse models of soft tissue sarcoma achieved over a 50% improvement in recurrence-free survival compared to resection of the tumor using direct visual guidance [19]. Since cathepsins are overexpressed in multiple types of solid tumors [17], similar techniques with combination of fluorescence guidance using LUM015 and conventional methods of screening and/or procedures could be potentially applied to target other primary and metastatic cancers such as CRC metastasis, ovarian and brain tumors [36-38], and contribute to more efficient procedures.

Although we tested the LUM015 probe in a variety of spontaneous and implanted mouse models of CRC, we did not evaluate the application of this probe in the wide spectrum of neoplastic colorectal disease. However, we used the mouse models that bear the most common genetic mutations found in the CRC to simulate the possible clinical scenarios for future clinical trials. Future studies focused on comprehensive pathological evaluation of human CRC samples with different grades, stages and various genetic mutations would be required to better guide patients selection for clinical trials that assess the real-time detection of colorectal lesions with fluorescence endoscopy using LUM015.

Recent advances in precision imaging approaches highlight the impact of image-guided procedures using smart probes with sophisticated chemical design that particularly target molecular signature of the tumors. Our study confirmed that cathepsin-activatable LUM015 probe has desirable characteristics for in-situ evaluation of colorectal tumors. Overexpression of cathepsins in CRC and real-time feedback during dual channel colonoscopy could bring the concept of optical molecular imaging guided diagnostic and therapeutic procedures closer to clinical use and provide valuable information to guide management decisions.

Acknowledgements

Disclosure of conflict of interest

J.M.F. is an employee at and has stock ownership from Lumicell, Inc. All other authors do not have relevant conflicts of interest. U.M. is a cofounder and consultant of CytoSite Biopharma, a company focused on development of PET probes for immuno-oncology.

Address correspondence to: Umar Mahmood, Athinoula A Martinos Center for Biomedical Imaging, Department of Radiology, Massachusetts General Hospital, Charlestown, MA, USA. Tel: 617-726-6477; Fax: 617-726-7422; E-mail: umahmood@mgh.harvard.edu

References

[1] Global Burden of Disease Cancer Collaboration, Fitzmaurice C, Allen C, Barber RM, Barregard L, Bhutta ZA, Brenner H, Dicker DJ, Chimed-Orchir O, Dandona R, Dandona L, Fleming

T, Forouzanfar MH, Hancock J, Hay RJ, Hunter-Merrill R, Huynh C, Hosgood HD, Johnson CO, Jonas JB, Khubchandani J, Kumar GA, Kutz M, Lan Q, Larson HJ, Liang X, Lim SS, Lopez AD, MacIntyre MF, Marczak L, Marquez N, Mokdad AH, Pinho C, Pourmalek F, Salomon JA, Sanabria JR, Sandar L, Sartorius B, Schwartz SM, Shackelford KA, Shibuya K, Stanaway J, Steiner C, Sun J, Takahashi K, Vollset SE, Vos T, Wagner JA, Wang H, Westerman R, Zeeb H, Zoeckler L, Abd-Allah F, Ahmed MB, Alabed S, Alam NK, Aldhahri SF, Alem G, Alemayohu MA, Ali R, Al-Raddadi R, Amare A, Amoako Y, Artaman A, Asayesh H, Atnafu N, Awasthi A, Saleem HB, Barac A, Bedi N, Bensenor I, Berhane A, Bernabe E, Betsu B, Binagwaho A, Boneya D, Campos-Nonato I, Castaneda-Orjuela C, Catala-Lopez F, Chiang P, Chibueze C, Chitheer A, Choi JY, Cowie B, Damtew S, das Neves J, Dey S, Dharmaratne S, Dhillon P, Ding E, Driscoll T, Ekwueme D, Endries AY, Farvid M, Farzadfar F, Fernandes J, Fischer F, G/Hiwot TT, Gebru A, Gopalani S, Hailu A, Horino M, Horita N, Husseini A, Huybrechts I, Inoue M, Islami F, Jakovljevic M, James S, Javanbakht M, Jee SH, Kasaeian A, Kedir MS, Khader YS, Khang YH, Kim D, Leigh J, Linn S, Lunevicius R, El Razek HMA, Malekzadeh R, Malta DC, Marcenes W, Markos D, Melaku YA, Meles KG, Mendoza W, Mengiste DT, Meretoja TJ, Miller TR, Mohammad KA, Mohammadi A, Mohammed S, Moradi-Lakeh M, Nagel G, Nand D, Le Nguyen Q, Nolte S, Ogbo FA, Oladimeji KE, Oren E, Pa M, Park EK, Pereira DM, Plass D, Qorbani M, Radfar A, Rafay A, Rahman M, Rana SM, Soreide K, Satpathy M, Sawhney M, Sepanlou SG, Shaikh MA, She J, Shiue I, Shore HR, Shrime MG, So S, Soneji S, Stathopoulou V, Stroumpoulis K, Sufiyan MB, Sykes BL, Tabares-Seisdedos R, Tadese F, Tedla BA, Tessema GA, Thakur JS, Tran BX, Ukwaja KN, Uzochukwu BSC, Vlassov VV, Weiderpass E, Wubshet Terefe M, Yebyo HG, Yimam HH, Yonemoto N, Younis MZ, Yu C, Zaidi Z, Zaki MES, Zenebe ZM, Murray CJL and Naghavi M. Global, regional, and national cancer incidence, mortality, years of life lost, years lived with disability, and disability-adjusted life-years for 32 cancer groups, 1990 to 2015: a systematic analysis for the global burden of disease study. JAMA Oncol 2017; 3: 524-548.

[2]   Blumenstein I, Tacke W, Bock H, Filmann N, Lieber E, Zeuzem S, Trojan J, Herrmann E and Schroder O. Prevalence of colorectal cancer and its precursor lesions in symptomatic and asymptomatic patients undergoing total colonoscopy: results of a large prospective, multicenter, controlled endoscopy study. Eur J Gastroenterol Hepatol 2013; 25: 556-561.

[3]   Cheng TI, Wong JM, Hong CF, Cheng SH, Cheng TJ, Shieh MJ, Lin YM, Tso CY and Huang AT.

Colorectal cancer screening in asymptomaic adults: comparison of colonoscopy, sigmoidoscopy and fecal occult blood tests. J Formos Med Assoc 2002; 101: 685-690.

[4]   Sheth RA and Mahmood U. Optical molecular imaging and its emerging role in colorectal cancer. Am J Physiol Gastrointest Liver Physiol 2010; 299: G807-820.

[5]   Habibollahi P, Waldron T, Heidari P, Cho HS, Alcantara D, Josephson L, Wang TC, Rustgi AK and Mahmood U. Fluorescent nanoparticle imaging allows noninvasive evaluation of immune cell modulation in esophageal dysplasia. Mol Imaging 2014; 13: 1-11.

[6]   Tummers QR, Verbeek FP, Schaafsma BE, Boonstra MC, van der Vorst JR, Liefers GJ, van de Velde CJ, Frangioni JV and Vahrmeijer AL. Real-time intraoperative detection of breast cancer using near-infrared fluorescence imaging and Methylene Blue. Eur J Surg Oncol 2014; 40: 850-858.

[7]   Sheth RA, Arellano RS, Uppot RN, Samir AE, Goyal L, Zhu AX, Gervais DA and Mahmood U. Prospective trial with optical molecular imaging for percutaneous interventions in focal hepatic lesions. Radiology 2015; 274: 917-926.

[8]   Blum G, von Degenfeld G, Merchant MJ, Blau HM and Bogyo M. Noninvasive optical imaging of cysteine protease activity using fluorescently quenched activity-based probes. Nat Chem Biol 2007; 3: 668-677.

[9]   Laxman B, Hall DE, Bhojani MS, Hamstra DA, Chenevert TL, Ross BD and Rehemtulla A. Noninvasive real-time imaging of apoptosis. Proc Natl Acad Sci U S A 2002; 99: 16551-16555.

[10]   Funovics MA, Alencar H, Montet X, Weissleder R and Mahmood U. Simultaneous fluorescence imaging of protease expression and vascularity during murine colonoscopy for colonic lesion characterization. Gastrointest Endosc 2006; 64: 589-597.

[11]   Hazen LG, Bleeker FE, Lauritzen B, Bahns S, Song J, Jonker A, Van Driel BE, Lyon H, Hansen U, Kohler A and Van Noorden CJ. Comparative localization of cathepsin B protein and activity in colorectal cancer. J Histochem Cytochem 2000; 48: 1421-1430.

[12]   Campo E, Munoz J, Miquel R, Palacin A, Cardesa A, Sloane BF and Emmert-Buck MR. Cathepsin B expression in colorectal carcinomas correlates with tumor progression and shortened patient survival. Am J Pathol 1994; 145: 301-309.

[13]   Tamhane T, Lllukkumbura R, Lu S, Maelandsmo GM, Haugen MH and Brix K. Nuclear cathepsin L activity is required for cell cycle progression of colorectal carcinoma cells. Biochimie 2016; 122: 208-218.

[14]   Talieri M, Papadopoulou S, Scorilas A, Xynopoulos D, Arnogianaki N, Platanioti G, Yotis J and

Agnanti N. Cathepsin B and cathepsin D expression in the progression of colorectal adenoma to carcinoma. Cancer Lett 2004; 205: 97-106.

[15] Van Noorden CJ, Jonges TG, Van Marle J, Bissell ER, Griffini P, Jans M, Snel J and Smith RE. Heterogeneous suppression of experimentally induced colon cancer metastasis in rat liver lobes by inhibition of extracellular cathepsin B. Clin Exp Metastasis 1998; 16: 159-167.

[16] Burden RE, Gormley JA, Jaquin TJ, Small DM, Quinn DJ, Hegarty SM, Ward C, Walker B, Johnston JA, Olwill SA and Scott CJ. Antibody-mediated inhibition of cathepsin S blocks colorectal tumor invasion and angiogenesis. Clin Cancer Res 2009; 15: 6042-6051.

[17] Whitley MJ, Cardona DM, Lazarides AL, Spasojevic I, Ferrer JM, Cahill J, Lee CL, Snuderl M, Blazer DG 3rd, Hwang ES, Greenup RA, Mosca PJ, Mito JK, Cuneo KC, Larrier NA, O'Reilly EK, Riedel RF, Eward WC, Strasfeld DB, Fukumura D, Jain RK, Lee WD, Griffith LG, Bawendi MG, Kirsch DG and Brigman BE. A mouse-human phase 1 co-clinical trial of a protease-activated fluorescent probe for imaging cancer. Sci Transl Med 2016; 8: 320ra4.

[18] Smith BL, Gadd MA, Lanahan CR, Rai U, Tang R, Rice-Stitt T, Merrill AL, Strasfeld DB, Ferrer JM, Brachtel EF and Specht MC. Real-time, intraoperative detection of residual breast cancer in lumpectomy cavity walls using a novel cathepsin-activated fluorescent imaging system. Breast Cancer Res Treat 2018; 171: 413-420.

[19] Lazarides AL, Whitley MJ, Strasfeld DB, Cardona DM, Ferrer JM, Mueller JL, Fu HL, Bartholf DeWitt S, Brigman BE, Ramanujam N, Kirsch DG and Eward WC. A fluorescence-guided laser ablation system for removal of residual cancer in a mouse model of soft tissue sarcoma. Theranostics 2016; 6: 155-166.

[20] Esfahani SA, Heidari P, Kim SA, Ogino S and Mahmood U. Optical imaging of Mesenchymal Epithelial Transition factor (MET) for enhanced detection and characterization of primary and metastatic hepatic tumors. Theranostics 2016; 6: 2028-2038.

[21] Martin ES, Belmont PJ, Sinnamon MJ, Richard LG, Yuan J, Coffee EM, Roper J, Lee L, Heidari P, Lunt SY, Goel G, Ji X, Xie Z, Xie T, Lamb J, Weinrich SL, VanArsdale T, Bronson RT, Xavier RJ, Vander Heiden MG, Kan JL, Mahmood U and Hung KE. Development of a colon cancer GEMM-derived orthotopic transplant model for drug discovery and validation. Clin Cancer Res 2013; 19: 2929-2940.

[22] Kucherlapati MH, Esfahani S, Habibollahi P, Wang J, Still ER, Bronson RT, Mahmood U and Kucherlapati RS. Genotype directed therapy in murine mismatch repair deficient tumors. PLoS One 2013; 8: e68817.

[23] Hung KE, Maricevich MA, Richard LG, Chen WY, Richardson MP, Kunin A, Bronson RT, Mahmood U and Kucherlapati R. Development of a mouse model for sporadic and metastatic colon tumors and its use in assessing drug treatment. Proc Natl Acad Sci U S A 2010; 107: 1565-1570.

[24] Sheth RA, Heidari P, Esfahani SA, Wood BJ and Mahmood U. Interventional optical molecular imaging guidance during percutaneous biopsy. Radiology 2014; 271: 770-777.

[25] Sheth RA, Upadhyay R, Weissleder R and Mahmood U. Real-time multichannel imaging framework for endoscopy, catheters, and fixed geometry intraoperative systems. Mol Imaging 2007; 6: 147-155.

[26] Hartgring SA, Willis CR, Bijlsma JW, Lafeber FP and van Roon JA. Interleukin-7-aggravated joint inflammation and tissue destruction in collagen-induced arthritis is associated with T-cell and B-cell activation. Arthritis Res Ther 2012; 14: R137.

[27] Chan AT, Baba Y, Shima K, Nosho K, Chung DC, Hung KE, Mahmood U, Madden K, Poss K, Ranieri A, Shue D, Kucherlapati R, Fuchs CS and Ogino S. Cathepsin B expression and survival in colon cancer: implications for molecular detection of neoplasia. Cancer Epidemiol Biomarkers Prev 2010; 19: 2777-2785.

[28] Bian B, Mongrain S, Cagnol S, Langlois MJ, Boulanger J, Bernatchez G, Carrier JC, Boudreau F and Rivard N. Cathepsin B promotes colorectal tumorigenesis, cell invasion, and metastasis. Mol Carcinog 2016; 55: 671-687.

[29] McIntyre RE, Buczacki SJ, Arends MJ and Adams DJ. Mouse models of colorectal cancer as preclinical models. Bioessays 2015; 37: 909-920.

[30] Segal E, Prestwood TR, van der Linden WA, Carmi Y, Bhattacharya N, Withana N, Verdoes M, Habtezion A, Engleman EG and Bogyo M. Detection of intestinal cancer by local, topical application of a quenched fluorescence probe for cysteine cathepsins. Chem Biol 2015; 22: 148-158.

[31] Clapper ML, Hensley HH, Chang WC, Devarajan K, Nguyen MT and Cooper HS. Detection of colorectal adenomas using a bioactivatable probe specific for matrix metalloproteinase activity. Neoplasia 2011; 13: 685-691.

[32] Hsiung PL, Hardy J, Friedland S, Soetikno R, Du CB, Wu AP, Sahbaie P, Crawford JM, Lowe AW, Contag CH and Wang TD. Detection of colonic dysplasia in vivo using a targeted heptapeptide and confocal microendoscopy. Nat Med 2008; 14: 454-458.

[33] Miller SJ, Joshi BP, Feng Y, Gaustad A, Fearon ER and Wang TD. In vivo fluorescence-based endoscopic detection of colon dysplasia in the mouse using a novel peptide probe. PLoS One 2011; 6: e17384.

[34] Gounaris E, Tung CH, Restaino C, Maehr R, Kohler R, Joyce JA, Ploegh HL, Barrett TA, Weissleder R and Khazaie K. Live imaging of cysteine-cathepsin activity reveals dynamics of focal inflammation, angiogenesis, and polyp growth. PLoS One 2008; 3: e2916.

[35] Garland M, Yim JJ and Bogyo M. A bright future for precision medicine: advances in fluorescent chemical probe design and their clinical application. Cell Chem Biol 2016; 23: 122-136.

[36] Moles A, Tarrats N, Fernandez-Checa JC and Marí M. Cathepsins B and D drive hepatic stellate cell proliferation and promote their fibrogenic potential. Hepatology 2009; 49: 1297-1307.

[37] Levicar N, Nuttall RK and Lah TT. Proteases in brain tumour progression. Acta Neurochir (Wien) 2003; 145: 825-838.

[38] Pranjol MZ, Gutowski N, Hannemann M and Whatmore J. The potential role of the proteases cathepsin D and cathepsin L in the progression and metastasis of epithelial ovarian cancer. Biomolecules 2015; 5: 3260-3279.